The Analysis of DC-link Voltage, Compensation range, Cost, Reliability and Power Loss for Shunt (Hybrid) Active Power Filters

Lei Wang[1], Chi-Seng Lam[2] and Man-Chung Wong[1,2]
1 - Department of Electrical and Computer Engineering, Faculty of Science and Technology, University of Macau, Macau, China
2 - State Key Laboratory of Analog and Mixed-Signal VLSI, University of Macau, Macau, China
E-mail: cslam@umac.mo / C.S.Lam@ieee.org

***Abstract*-The design of shunt active power filters (APFs) and hybrid active power filters (HAPFs) with desirable characteristics are the major trend in the future, such as wide compensation range, high reliability, low cost, low switching loss, good tacking performance, etc. Over the past few decades, significant researches were focused on addressing the technical challenges associated with the parameter design, operation and control of the APFs and HAPFs. However, the comprehensive review of DC-link voltage, compensation range, cost, reliability, power loss and tracking performance has been barely studied. Therefore, the intent of this paper is to provide a clear picture of the selection of APFs and HAPFs based on DC-link voltage, compensation range, cost, reliability and power loss. The supreme one will be selected among different APFs and HAPFs by considering the DC-link voltage, compensation range, cost, reliability and power loss. Finally, the simulation results of different APFs and HAPFs will be provided to verify their compensation performances.**

***Index Terms*—V-I characteristic, cost, reliability, power loss for shunt active power filters (APFs), hybrid active power filters (HAPFs)**

I. INTRODUCTION

INSTALLATION of the current quality compensators is one of the solutions for different power quality problems. The historical review of different power quality compensators are summarized in Table I and compared in the following.

Shunt capacitor banks (CBs) are firstly applied in power systems since 1900s for power-factor correction and feeder voltage control. However, CBs easily get burnt if the current harmonics level is high. To compensate the current harmonics, the passive power filters (PPFs) are proposed in 1940s. Unfortunately, the PPFs have many disadvantages like low dynamic performance, resonance problem, etc [1]. The static var compensators (SVCs) were proposed in 1960s for dynamic reactive power compensation [2]. However, the SVCs suffer drawbacks such as resonance problem, harmonic current injection and poor harmonic compensation ability. To overcome those drawbacks of SVCs and improve performance simultaneously, the active power filters (APFs) were proposed in the year of 1976 [3],[4]. Unfortunately, APFs still cannot large scale development in the markets due to the high initial and operational costs. Afterwards, the *LC*-coupling hybrid active filters (HAPFs) were proposed in the year of 2003 with lower active inverter rating [5], [6]. Since the active inverter rating is proportional to the cost of compensators, the HAPFs are more cost-effective than APFs. However, the HAPFs have a narrow compensation range, which limits its compensation ability. From 2014 onwards, the thyristor controlled *LC*-coupling hybrid active power filter (TCLC-HAPF) has been widely studied in [7]-[13], which has the characteristics of a wider compensation range than HAPF and smaller DC-link voltage than APF for power quality compensation.

Table I Characteristics of different active current quality compensators

Year	1900s	1940s	1960s	1976	2003	2014
Compensators	CBs	PPFs	SVCs	APFs	HAPFs	TCLC-HAPF
Compensation Range	*	*	***	****	*	****
Harmonics Compensation	*	**	*	****	****	****
Cost	*	*	**	****	***	***
Reliability	****	****	***	*	**	***
Switching loss	*	*	**	****	***	**
Tacking performance	*	*	***	****	**	****

*Notes: The shaded area means undesirable characteristics and more * means stronger of characteristic which will be discussed in this paper.*

Based on above discussions and Table I, the traditional power quality compensators CBs, PPFs and SVCs have poor harmonic compensation performance. The poor performance problem can be solved if the active inverter part has been added to the topologies such as APFs, HAPFs and TCLC-HAPFs. This paper aims to compare the APFs, HAPFs and TCLC-HAPFs in terms of DC-link voltage, compensation range, cost, reliability, power loss and tracking performance.

The layout of this paper can be described as following. First of all, the structures of APF, HAPF and TCLC-HAPF will be introduced in section II. Then, the comparisons among different power quality compensators will be given in terms of DC-link voltage, compensation range (section III) cost (section IV), reliability (section V) and power loss (section VI). The simulation results are provided in section VII to verify the DC-link voltage, compensation range and tracking performance and compensation performances of APF, HAPF and TCLC-HAPF. The experimental results are provided in

Project Supported in part by the Science and Technology Development Fund, Macao SAR (FDCT) (025/2017/A1, 109/2013/A3) and in part by the Research Committee of the University of Macau (MYGR2017-00038-FST, MYRG2015-00009-FST and MYRG2017-00090-AMSV)

section VIII for the most preferable compensator TCLC-HAPF. Finally, the summary will be drawn in section IX.

II. Structures of APF, HAPF and TCLC-HAPF

Fig. 1 and Fig. 2 show the structures of APF, HAPF and TCLC-HAPF, in which the subscript "*x*" stands for phase *a*, *b,* and *c* in the following analysis. v_{sx} and v_x are the source and load voltages; i_{sx}, i_{Lx}, and i_{cx} are the source, load, and compensating currents, respectively. L_s is the transmission line impedance.

For low voltage level applications, the two-level power quality compensators as shown in Fig. 1 can be used to solve power quality issues. For the high voltage applications, both coupling *LC* part of HAPF and TCLC part of TCLC-HAPF can provide large voltage drops, so that the DC-link voltages can be significantly reduced. However, when the voltage level is higher than the maximum rating of power switches, the cascade multilevel technique can be applied to reduce the high voltage stress across each power switch and DC-link capacitor as shown in Fig. 2.

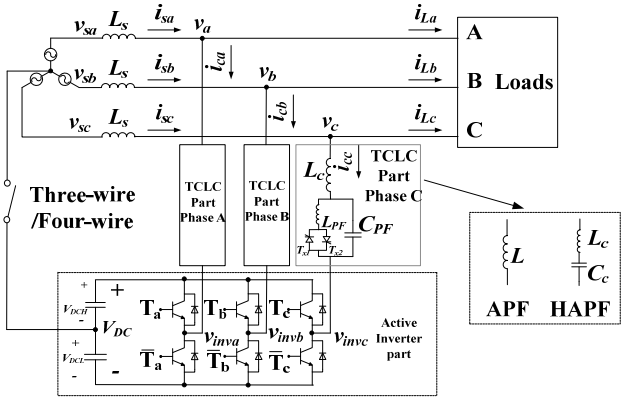

Fig. 1 Structures of two-level APF, HAPF and TCLC-HAPF

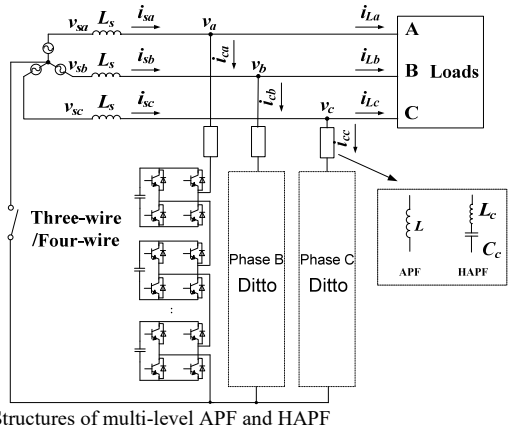

Fig. 2. Structures of multi-level APF and HAPF

III. DC-link Voltage and Compensation Range of APF, HAPF and TCLC-HAPF

Based on the structures given in Fig. 1, the DC-link voltage and compensation range of APF, HAPF and TCLC-HAPF are compared and discussed.

At the fundamental frequency, based on Fig. 1, the equations for APF and HAPF can be obtained as:

$$V_{invx\,1(APF)} = \left|V_{x1} + X_{L1}\cdot I_{Lxq\,1}\right| = V_{x1}\cdot\left|\frac{V_{x1}^2/X_{L1} - V_{x1}I_{Lxq\,1}}{V_{x1}^2/X_{L1}}\right| = V_{x1}\cdot\left|\frac{Q_{cx\_L} + Q_{Lxf}}{Q_{cx\_L}}\right| \quad (1)$$

$$V_{invx\,1(HAPF)} = V_{x1}\cdot\left|\frac{Q_{cx\_LC} - Q_{Lxf}}{Q_{cx\_LC}}\right| \quad (2)$$

$$V_{invx\,1(TCLC-HAPF)} = V_{x1}\cdot\left|\frac{Q_{cx\_TCLC} - Q_{Lxf}}{Q_{cx\_TCLC}}\right| \quad (3)$$

where Q_{Lx1}, Q_{cx_L}, Q_{cx_LC} and Q_{cx_TCLC} can be expressed as:

$$Q_{Lx1} = V_{x1}\cdot I_{Lxq1} \quad (4)$$

$$Q_{cx\_L} = V_{x1}^2/\omega L \quad (5)$$

$$Q_{cx\_LC} = V_{x1}^2/(\omega L_c - 1/\omega C_c) \quad (6)$$

$$Q_{cx\_TCLC} = \frac{V_{x1}^2}{\frac{\pi\omega L_{PF}}{(2\pi - 2\alpha + \sin 2\alpha) - \pi\omega^2\cdot L_{PF}C_{PF}} + \omega L_c} \quad (7)$$

where ω is angular frequency, I_{Lxq1} is the reactive power component of the load current, L is the coupling inductor of APF, L_c and C_c are the coupling capacitor and inductor of the HAPF, respectively. For the harmonic frequency, the inverter voltage can be expressed as:

$$V_{invxn(APF)} = n\omega L\cdot I_{Lxn} \quad (8)$$

$$V_{invxn(HAPF)} = \left|n\omega L_c - 1/n\omega C_c\right|\cdot I_{Lxn} \quad (9)$$

$$V_{invxn(HAPF)} = \left|\frac{\pi(n\omega L_{PF})}{(2\pi - 2\alpha + \sin 2\alpha) - \pi(n\omega)^2\cdot L_{PF}C_{PF}} + n\omega L_c\right|\cdot I_{Lxn} \quad (10)$$

and I_{Lxn} is the load harmonic current. And the DC-link voltage can be expressed as:

$$V_{DC} = \sqrt{6\cdot V_{invx1}^2 + 6\cdot\sum_{n=2}^{\infty} V_{invxn}^2} \quad (11)$$

where the V_{invx1} can be found from (1)-(3) and V_{invxn} can be found from (8)-(11). Based on above analysis, the DC-link voltage in terms of reactive power and harmonic current can be provided as Fig. 3. And the parameters are from Table II.

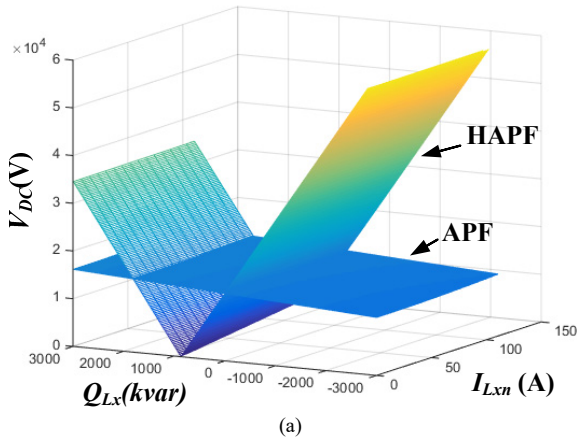

(a)

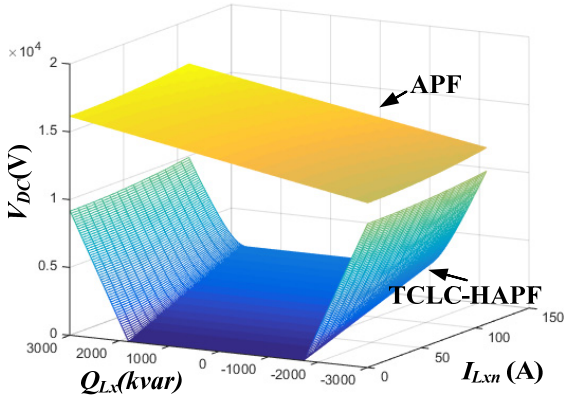

(b)

Fig. 3 DC-link voltage in terms of reactive power and harmonic current (a) APF and HAPF (b) APF and TCLC-HAPF

Table II Simulation and Experimental Parameters for APF, HAPF and TCLC-HAPF

	Parameters	Physical values
System parameters	V_{LL}, f, L_s	*10kV, 50Hz,0.1mH*
APF	L	*5mH*
HAPF	L, C	*2.5mH, 80uF*
TCLC-HAPF	L_c, L_{PF}, C_{PF}	*2.5mH, 30mH,160uF*

Based on Fig. 3, the below conclusions can be drawn as:

1) The required V_{DC} of APF is large due to the small coupling impedance X_L.
2) The HAPF has a low DC-link voltage characteristic only within a narrow inductive load range. When the load reactive power is outside its designed range, the HAPF requires a high DC-link operating voltage (>10kV) due to its large coupling capacitor impedance, and thus it easily loses its low voltage rating advantage.
3) The TCLC-HAPF has the desirable characteristic of a wide compensation range (from capacitive to inductive reactive power) with a low DC-link voltage.

IV. Cost Comparison among APF, HAPF and TCLC-HAPF

In this part, the cost study of APF, HAPF and TCLC-HAPF will be provided. For cost study, many aspects need to be considered as below [14]-[16]: a) field construction cost, b) auxiliary components cost, c) magnetic components cost, d) passive components cost and e) solid-state devices cost. Each aspect has its corresponding portion of total cost. However, in the industrial market, the cost of PPF, SVC and APF in terms of power rating are available in [15], [16] (shown as Fig. 4(a)-(b)). Even the detail cost of HAPF and TCLC-HAPF are not easily be found, the cost of HAPF and TCLC-HAPF can be approximately calculated by using the cost PPF, SVC and APF [15], [16].

The HAPF can be considered as the PPF in series with APF. However, the required rating of active inverter part of HAPF is much lower than APF. The cost of HAPF can be approximately calculated as:

$$Cost_{HAPF} = k_{HAPF} \cdot Cost_{APF} + Cost_{PPF} \quad (12)$$

where $Cost_{APF}$ and $Cost_{PPF}$ are the costs of APF and PPF, respectively, which can be observed from Fig. 4(a)-(b). The k_{HAPF} is the power ratio of active inverter part between HAPF and APF. If the k_{HAPF} is small enough, the HAPF is cheaper than APF. The capacity of the active inverter part (or DC-link voltage) of HAPF is only k_{HAPF}=27% of the capacity of the APF.

On the other hand, the TCLC-HAPF can be considered as the SVC part (TCLC part) in series with active inverter part. The cost of TCLC-HAPF can be approximately calculated as:

$$Cost_{TCLC-HAPF} = k_{TCLC-HAPF} \cdot Cost_{APF} + Cost_{SVC} \quad (13)$$

where $Cost_{APF}$ and $Cost_{SVC}$ are the costs of APF and SVC respectively. The $k_{TCLC-HAPF}$ is the power ratio of active inverter part between TCLC-HAPF and APF. The capacity of the active inverter part (or DC-link voltage) of proposed TCLC-HAPF is only $k_{TCLC-HAPF}$=17% of the capacity of the APF for wide range compensation (both inductive and capacitive).

Based on (12), (13) and the cost study in [15], [16], the costs of the PPF, SVC, APF, HAPF and TCLC-HAPF can be plotted as Fig. 4.

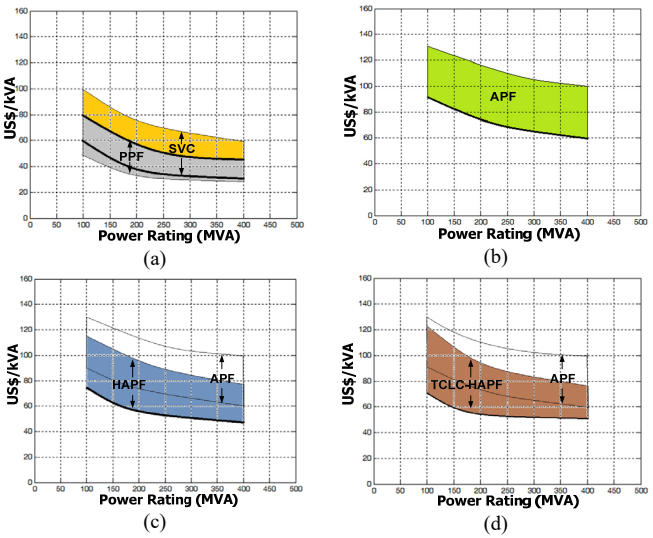

(a) (b) (c) (d)

Fig. 4 Typical high voltage investment costs for (a) PPF and SVC (b) APF, (c) HAPF, (d) TCLC-HAPF

In Fig. 4, there are two limit lines for each compensator. The lower limit cost line indicates the equipment costs, while the upper limit means the total investment costs. It is clearly shown that at low power rating, the costs per MAV are higher than at the high power rating. By comparing the costs in Fig. 4, it can be seen that the cost of both HAPF and TCLC-HAPF are around 7.7% ~ 23% cheaper than the APF for high voltage level applications.

V. Reliability Comparison Among APF, HAPF and TCLC-HAPF

In order to have a high-quality performance, all of the components of power quality compensators are required to work safely and well-functioning. In the practical systems, all of the components have specific failure rate and repair/replacement time. Among them, the switching components like IGBTs and thyristors have the highest failure rates, so that only switching components are focused for the comparison. In the following, the reliability comparison among

APF, HAPF and TCLC-HAPF under a medium voltage application (10kV) is discussed.

For a medium 10kV voltage application, as shown in section VII, the minimum required DC-link voltage of APF is about 15kV, which is larger than any existed IGBT voltage rating, so that the APF requires multi-level structures in Fig. 2 to reduce the high voltage stress across each power switch and DC-link capacitor. In contrast, the required DC-link voltage of HAPF and TCLC-HAPF are around 4.0 kV (27% of APF rating) and 2.6 kV (17% of APF rating), respectively. For comparison, the same voltage level 3kV is used for DC-link capacitor, IGBTs in active inverter parts of APF, HAPF and TCLC-HAPF. Therefore, the HAPF and APF require two stages and five stages multilevel structures, respectively. And total required switching components of HAPF and APF are 24 and 60. As for TCLC-HAPF, the total required switching component is just 12. Considering the system will work if and only if all the components are functioning well, the system reliability can then be roughly calculated as [17]-[20]:

$$Re_{tot} = e^{-\lambda_{tot} t} \tag{14}$$

where Re_{tot} and λ_{tot} are the total reliability and total failure rate of system. The λ_{tot} is the sum of different components as shown in Table III.

Table III The failure rate of each component in power quality compensators [19]-[20]

Component	λ_p (failure/10^6hours)	APF	HAPF	TCLC-HAPF
IGBT	$\lambda_{p(IGBT)}$=12.0	720 (n=60)	288 (n=24)	72 (n=6)
Thyristor	$\lambda_{p(Thyristor)}$=16.4	0	0	98.4 (n=6)
AC inductor	$\lambda_{p(L)}$ =0.0718	0.215 (n=3)	0.215 (n=3)	0.215 (n=3)
AC capacitor	$\lambda_{p(C)}$ =1.25	0	3.75 (n=3)	3.75 (n=3)
DC-link capacitor	$\lambda_{P(C\_DC)}$ =0.102	1.52 (n=15)	0.612 (n=6)	0.204 (n=2)
Whole System	λ_{tot}	721.7	292.6	174.46

The detailed calculations in above Table III can be found from [18]-[20]. Based on all above analysis and summarized Table III, the system reliability of APF, HAPF and TCLC-HAPF can be plotted as Fig. 5.

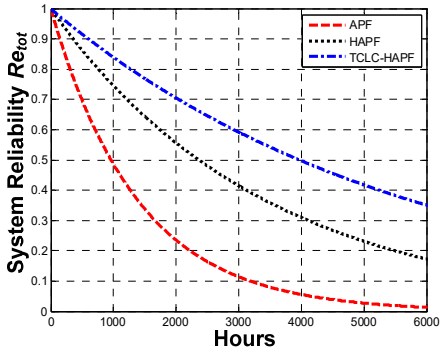

Fig. 5 The system reliability of APF, HAPF and TCLC-HAPF

From Fig. 5, it can be clearly observed that the TCLC-HAPF has much higher reliability than the multilevel HAPF and APF. Therefore, the potential maintenance time and costs of TCLC-HAPF can be significantly reduced.

VI. Power Loss Comparison among APF, HAPF and TCLC-HAPF

The power loss of the APF, HAPF and TCLC-HAPF are mainly from switching loss of IGBTs and/or thyristors. Therefore, the switching loss is focused in this paper.

The switching loss of the APF and HAPF are from the switching components (IGBTs) in active inverter part. In contrast, the switching loss of the TCLC-HAPF consists of two parts: 1) switching loss from IGBTs in active inverter and 2) switching loss from thyristors in part TCLC.

The total turn-on and turnoff switching loss from IGBTs in active inverter can be calculated as [21]:

$$P_{sw(IGBT)} = V_{DC} I_{CM} f_{sw} \left(\frac{1}{8} t_{rN} \frac{I_{CM}^2}{I_{CN}} + t_{fN} \left(\frac{1}{3\pi} + \frac{1}{24} \cdot \frac{I_{CM}}{I_{CN}} \right) \right) \tag{15}$$

where V_{DC}, I_{CM}, I_{CN}, t_{rN}, t_{fN}, and f_{sw} are the DC-link voltage, maximum collector current, rated collector current, rated rise time, rated fall time, and switching frequency, respectively.

Each thyristor in TCLC part only turn on one time in a fundamental period which is different with IGBTs in active inverter part. In TCLC-HAPF applications, the on-state switching loss is the dominate part for thyristors that can be easily calculated as [22]:

$$P_{sw(thyristor)} = U_{TO} \times I_{TAV} + r_T \times I_{TRMS}^2 \tag{16}$$

where I_{TRMS} is the RMS value of current passing though thyristor, I_{TAV} is the average value of current passing though thyristor, U_{TO} is the thyristor threshold voltage and r_T is the thyristor slope resistance.

In 10kV system, the 3.3kV IGBT modules (FZ1000R33HL3) are selected for active inverter parts of multilevel APF, HAPF and TCLC-HAPF. Meanwhile, the 8kV thyristor modules (T1901N [26]) are used for TCLC part of TCLC-HAPF. The parameters' values of IGBT modules (FZ1000R33HL3 [27]) and thyristor modules (T1901N) are provided in Table IV.

Table IV The parameters' values of IGBT modules (FZ1000R33HL3) and thyristor modules (T1901N)

t_{rn}	0.55us	V_{DC}	2600V	r_T	0.44mΩ
t_{fn}	0.40us	I_{CN}	1000A	U_{TO}	1.24V
f_{sw}	5kHz	I_{CM} =I_{TRMS} = I_{TAV}=I_{cx}			

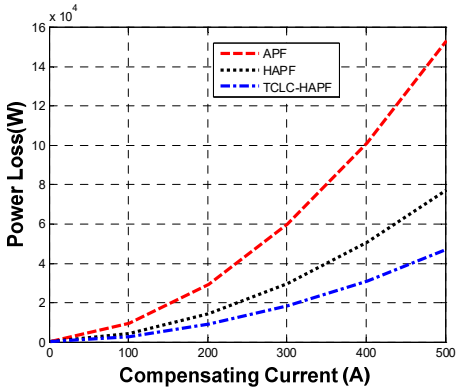

Fig. 6 The power loss of APF, HAPF and TCLC-HAPF

From Fig. 6, it can be clearly observed that the TCLC-HAPF has much lower power loss than the multilevel HAPF and APF.

VII. Simulation Results

The purpose of experimental results is to verify the DC-link voltage, compensation range and tracking performance and compensation performances of APF, HAPF and TCLC-HAPF. The parameter used for simulation is provided in Table II.

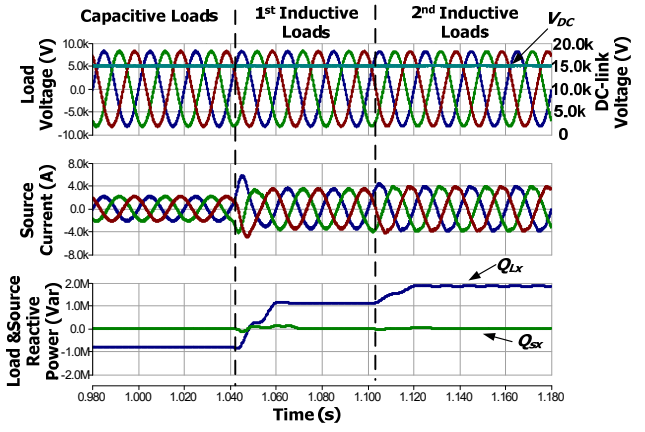

(a)

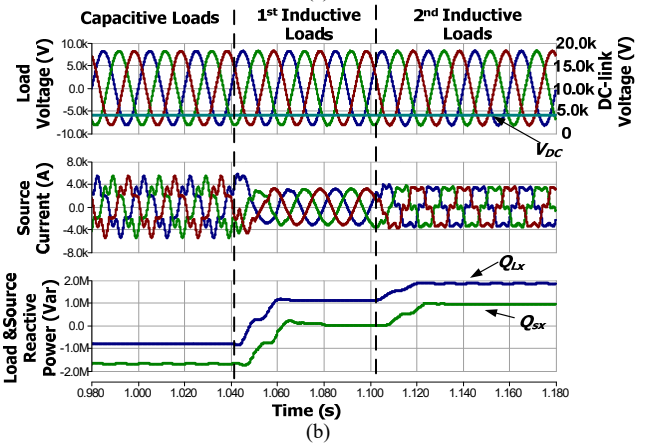

(b)

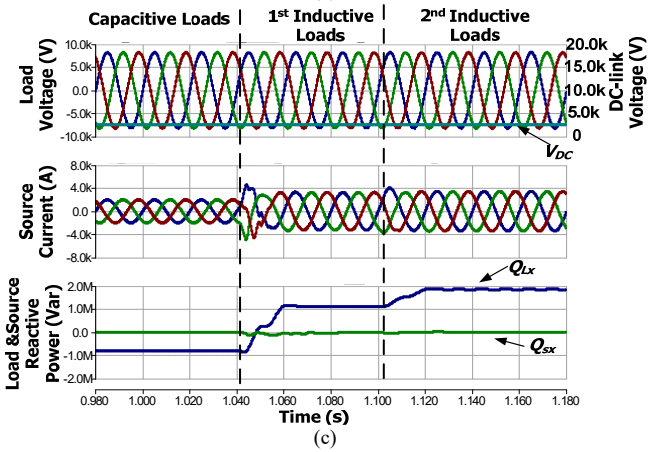

(c)

Fig. 7. Dynamic compensation waveforms of load voltage, DC-link voltage, source current, and load and source reactive powers by applying: (a) APF, (b) HAPF and (c) TCLC-HAPF in different loadings cases

Based on Fig. 7 (a) and Table V, the APF can provided wide compensation range with high DC-link voltage V_{DC_tot}= 15kV. For the different loads compensations, the APF can provide satisfactory power factor (PF) and source current THD_{isx} performance. After APF compensation, the *PF* is improved to ≥ 0.99 and THD_{isx} ≤ 4.2%.

From Fig. 7(b) and Table V, the HAPF can only compensate narrow range of reactive power (just matches with the 1st inductive loads case). However, the HAPF cannot provide satisfactory source side PF and current compensation results when the reactive power is capacitive or outside its inductive compensation range. Specifically, the *PF* and THD_{isx} are 0.86 and 22.0% for the 2nd inductive loads compensation. And the *PF* and THD_{isx} are 0.62 and 26.6% for the capacitive loads compensation.

From Fig. 7(c) and Table V, the TCLC-HAPF can provide wide reactive power compensation range (from inductive to capacitive). After proposed TCLC-HAPF compensation, the source reactive power is reduced to around zero in different loads cases. And the PF and THD_{isx} are compensated to unity and ≤ 4.0% respectively for the different loads.

Based on Fig. 7, the TCLC-HAPF has low DC-link voltage, wide compensation range, good tracking performance among the different compensators.

Table V Simulation results by using APF, HAPF and TCLC-HAPF

Load Type	Compensator	I_{sx}(A)	I_{cx}(A)	*PF*	$THDi_{sx}$(%)	V_{DC}(V)	S_{inv}(VA)
Case *A:* 1st inductive loads	Before Comp.	340	--	0.83	0.1	--	--
	APF	308	178	0.99	2.9	15.0k	4.62M
	HAPF	282	180	0.99	3.0	4.0k	1.25M.
	TCLC-HAPF	290	184	1.00	2.4	2.5k	0.8M
Case *B:* 2nd inductive loads	Before Comp.	440	--	0.69	0.1	--	--
	APF	320	300	0.99	5.0	15.0k	7.80M
	HAPF	315	180	0.86	22.0	4.0k	1.25M
	TCLC-HAPF	300	303	1.00	1.9	2.5k	1.31M
Case *C:* Capacitive loads	Before Comp.	225	--	0.78	0.1	--	--
	APF	192	132	1.00	4.2	15.0k	3.43M
	HAPF	372	180	0.62	26.5	4.0k	1.27M
	TCLC-HAPF	181	132	1.00	4.0	2.5k	0.57M

**Shaded areas indicate undesirable results.*

VIII. Experimental Results

The experimental results aim to verify the DC-link voltage characteristics, tracking performances and compensation performances of the TCLC-HAPF. The three-phase three-wire 110V-5kVA TCLC-HAPF experimental prototypes are constructed in the laboratory as shown in Fig. 8.

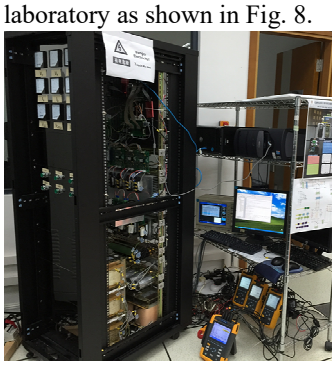

Fig. 8 The 110V-5kVA SVC-HAPF experimental prototype and its testing environment

Fig. 9 shows the experimental performance of TCLC-HAPF. From Fig. 9, it can be seen that the experimental PF and THD_{isx} can be improved to 0.99, 6.3% (the worst phase) for the 1st load compensation. And the experimental PF and THD_{isx} are

improved to 0.90, 5.5% (the worst phase) for the 1st and 2nd loads compensation. To compensation both loads, the HAPF required DC-link voltage is about 60V.

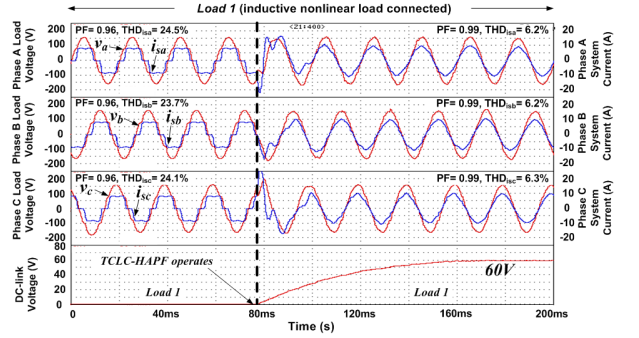

Fig. 9. Waveforms of source current, natural current and DC-link voltage: (a) before and after TCLC-HAPF starts operation during 1st load and (b) when 2nd load is connected.

IX. Conclusion

In this paper, the comparisons among the APF, HAPF and TCLC-HAPF have been provided in terms of DC-link voltage, compensation range, cost, reliability and power loss. The discussions and comparison results have been summarized as Table I. Compared TCLC-HAPF with APF and HAPF, it has higher reliability and lower power loss than both APF and HAPF. Besides, the TCLC-HAPF can be more cost effective than APF for medium/high voltage level applications. In addition, the TCLC-HAPF has the wider compensation range than HAPF and lower DC-link voltage than APF and HAPF. Therefore, the TCLC-HAPF has the large potential to be further developed for medium/high voltage level applications.

Reference

[1] J. C. Das, "Passive filters—Potentialities and limitations," *IEEE Trans. Ind. Appl.,* vol. 40, no. 1, pp. 232–241, Jan./Feb. 2004.

[2] L. Wang, C. S. Lam, and M. C. Wong, "Design of A thyristor controlled LC compensator for dynamic reactive power compensation in smart grid," *IEEE Trans. Smart. Grid*. vol. 8, no. 1, pp. 409-417, Jan. 2017.

[3] S. D. Swain, P. K. Ray and K. B. Mohanty, "Improvement of Power Quality Using a Robust Hybrid Series Active Power Filter," *IEEE Trans. Power Electron.*, vol. 32, no. 5, pp. 3490-3498, May 2017.

[4] J. Fang, G. Xiao, X. Yang and Y. Tang, "Parameter Design of a Novel Series-Parallel-Resonant LCL Filter for Single-Phase Half-Bridge Active Power Filters," *IEEE Trans. Power Electron.*, vol. 32, no. 1, pp. 200-217, Jan. 2017.

[5] L. Wang, C. S. Lam, M. C. Wong *et al,* "Non-linear adaptive hysteresis band pulse-width modulation control for hybrid active power filters to reduce switching loss," *IET. Power Electron*, vol. 8, no. 11, pp. 2156-2167, Nov. 2015.

[6] K. W. Lao, M. C. Wong, *et al.* "Analysis in the Effect of Co-phase Traction Railway HPQC Coupled Impedance on Its Compensation Capability and Impedance-Mapping Design Technique Based on Required Compensation Capability for Reduction in Operation Voltage," *IEEE Trans. Power Electron.* vol. 32, no. 4, pp. 2631-2646, Apr. 2017.

[7] L. Wang, C. S. Lam, and M. C. Wong, "A hybrid-STATCOM with wide compensation range and low dc-link voltage," *IEEE Trans. Ind. Electron.,* vol. 63, no. 6, pp. 3333-3343, Jun. 2016.

[8] S. Rahmani, A. Hamadi, and K. Al-Haddad, "A combination of shunt hybrid power filter and thyristor-controlled reactor for power quality," *IEEE Trans. Ind. Electron.,* vol. 61, no. 5, pp. 2152 - 2164, May 2014.

[9] L. Wang, C. S. Lam, and M. C. Wong "An unbalanced control strategy for a thyristor controlled LC-coupling hybrid active power filter (TCLC-HAPF) in Three-phase Three-wire Systems," *IEEE Trans. Power Electron.*, vol. 32, no. 2, pp. 1056-1069, Feb. 2017.

[10] L. Wang, C. S. Lam, and M. C. Wong, "Analysis, Control and Design of Hybrid Grid-Connected Inverter for Renewable Energy Generation with Power Quality Conditioning," *IEEE Trans. Power Electron.,* vol. 33, no. 8, pp. 6755-6768, Aug. 2018

[11] L. Wang, C. S. Lam, M. C. Wong, "Modeling and parameter design of thyristor controlled LC-coupled hybrid active power filter (TCLC-HAPF) for unbalanced compensation," *IEEE Trans. Ind. Electron.*, vol. 64, no. 3, pp. 1827-1840, March 2017

[12] C. S. Lam; L. Wang; S. I. Ho; M. C. Wong, "Adaptive Thyristor Controlled LC – Hybrid Active Power Filter for Reactive Power and Current Harmonics Compensation with Switching Loss Reduction," *IEEE Trans. Power Electron.*, early access, doi: 10.1109/TPEL.2016.2640304

[13] L. Wang; C. S. Lam; M. C. Wong, "Selective Compensation of Distortion, Unbalanced and Reactive Power of a Thyristor Controlled LC-Coupling Hybrid Active Power Filter (TCLC-HAPF)," *IEEE Trans. Power Electron.*, vol. 32, no. 12, pp. 9065-9077, Dec. 2017

[14] C. Kawann, A.E. Emanuel, "Passive shunt harmonic filters for low and medium voltage: a cost comparison study." *IEEE Trans. Power Syst.*, vol.11, no.4, pp.1825-1831, Nov 1996

[15] K. Habur and D. O'Leary, "FACTS – For cost effective and reliable transmission of electrical energy." [Online]. Available: http://www.worldbank.org/html/fpd/em/transmission/facts_siemens.pdf

[16] L. M. Tolbert, T. J. King, et al. "Power electronics for distributed energy systems and transmission and distribution applications: Assessing the technical needs for utility applications," ORNL/TM-2005/230, Oak Ridge Nat. Lab., Dec. 2005.

[17] F. Richardeau and T. T. L. Pham, "Reliability Calculation of Multilevel Converters: Theory and Applications," *IEEE Trans. Ind. Electron.*, vol. 60, no. 10, pp. 4225-4233, Oct. 2013.

[18] X. Yu and A. M. Khambadkone, "Reliability Analysis and Cost Optimization of Parallel-Inverter System," *IEEE Trans. Ind. Electron.*, vol. 59, no. 10, pp. 3881-3889, Oct. 2012.

[19] B. Abdi, A. H. Ranjbar, G. B. Gharehpetian and J. Milimonfared, "Reliability Considerations for Parallel Performance of Semiconductor Switches in High-Power Switching Power Supplies," *IEEE Trans. Ind. Electron.*, vol. 56, no. 6, pp. 2133-2139, June 2009.

[20] Reliability Prediction of Electronic Equipments (MIL-HDBK-217), Relex Software Corporation, Greensburg, PA, 1990.

[21] M.-C. Wong, J. Tang, and Y.-D. Han, "Cylindrical coordinate control of three-dimensional PWM technique in three-phase four-wired trilevel inverter," *IEEE Trans. Power Electron.,* vol. 18, no. 1, pp. 208–220, Jan. 2003

[22] E. Baussan, E. Bouquerel, M. Dracos, et al. "Study of the pulse power supply unit for the four-horn system of the CERN to Frejus neutrino super beam", *Journal of Instrum.*, T07006. Aug. 2013

[23]Z. Dang and J. A. Abu Qahouq, "Evaluation of High-Current Toroid Power Inductor With NdFeB Magnet for DC–DC Power Converters," *IEEE Trans. Ind. Electron.,* vol. 62, no. 11, pp. 6868-6876, Nov. 2015.

[24]A. Braham, A. Lahyani, P. Venet and N. Rejeb, "Recent Developments in Fault Detection and Power Loss Estimation of Electrolytic Capacitors," *IEEE Trans. Power Electron.,* vol. 25, no. 1, pp. 33-43, Jan. 2010.

[25]X. S. Pu, T. H. Nguyen, D. C. Lee, K. B. Lee and J. M. Kim, "Fault Diagnosis of DC-link Capacitors in Three-Phase AC/DC PWM Converters by Online Estimation of Equivalent Series Resistance," *IEEE Trans. Ind. Electron.,* vol. 60, no. 9, pp. 4118-4127, Sept. 2013.

[26] Infineon Technologies AG: http://www.infineon.com/ Datasheet: T1901N (2011). [Online]. Available: http://www.infineon.com/eupec

[27] Infineon Technologies AG: http://www.infineon.com/ Datasheet: FZ1000R33HL3 (2013). Available at: http://www.infineon.com/eupec